Simulation and Application of a Piezo-Driven System Enabling Vibration-Assisted Micro Milling

Sebastian Greco[1]
Institute for Manufacturing Technology and Production Systems,
Technische Universität Kaiserslautern, Germany

Katja Klauer
Institute for Manufacturing Technology and Production Systems,
Technische Universität Kaiserslautern, Germany

Benjamin Kirsch
Institute for Manufacturing Technology and Production Systems,
Technische Universität Kaiserslautern, Germany

Jan C. Aurich
Institute for Manufacturing Technology and Production Systems,
Technische Universität Kaiserslautern, Germany

Abstract

The ongoing miniaturization of components and the functionalization of surfaces necessitates the improvement of micro machining processes and to increase their efficiency. One method to increase the machining efficiency is reducing the process forces and tool wear, which is achieved by the implementation of vibration-assisted cutting in conventional machining processes. In vibration-assisted cutting, the conventional cutting movement is superimposed by a vibration with defined frequency. By using vibration-assisted cutting technologies, besides increased efficiency, a wider range of materials can be machined. In this paper, vibration-assisted cutting is transferred to micro machining. For this purpose, the design, simulation and application of an easy to integrate system that enables vibration-assisted cutting for micro machining processes is described. The setup was tested using a micro milling process. Two orientations between feed direction and vibration direction were investigated. Frequencies up to 15 kHz were examined, the machined material was brass (CuZn39Pb2). The effect of the superimposed vibration was analysed on the basis of process force, surface roughness, burr formation and slot bottom and was compared with the process results of micro milling without vibration-assistance. A decrease in process forces of up to 63 % was observed during vibration-assisted micro milling.

2012 ACM Subject Classification Applied computing → Physical sciences and engineering

Keywords and phrases micro machining, micro milling, vibration-assisted cutting, Finite Element Analysis, surface roughness

Digital Object Identifier 10.4230/OASIcs.iPMVM.2020.3

Funding The authors would like to thank the German research foundation (DFG) for the financial support within the project AU 185/57-1 "Ultrasonic air bearing spindle for micro machining". Also funded by the Deutsche Forschungsgemeinschaft (DFG, German Research Foundation) - project number 172116086 - SFB 926.

[1] corresponding author

2nd International Conference of the DFG International Research Training Group 2057 – Physical Modeling for Virtual Manufacturing (iPMVM 2020).
Editors: Christoph Garth, Jan C. Aurich, Barbara Linke, Ralf Müller, Bahram Ravani, Gunther Weber, and Benjamin Kirsch; Article No. 3; pp. 3:1–3:18

OpenAccess Series in Informatics
OASICS Schloss Dagstuhl – Leibniz-Zentrum für Informatik, Dagstuhl Publishing, Germany

1 Introduction

The ongoing miniaturization of components and assemblies as well as the functionalization of surfaces used for example in electro mechanical instruments or medical devices [4] lead to a demand for increasing the efficiency and accuracy of micro machining processes. Microstructures, which are essential for such applications, are typically dimensioned significantly smaller than one millimeter. One possibility to produce such filigree structures is the application of micro milling processes with tool diameters smaller 100 µm [1]. Analogous to the machining of larger structures, the accuracy of the micro milling processes is dependent on the machine tool's stiffness [7], arising tool wear and resulting surface quality. In addition, lower tool wear also results in lower process forces [14]. For these reasons and since vibration-assisted machining reduces process forces and tool wear, vibration-assisted machining can be used to significantly increase the accuracy and efficiency of the machining result.
During vibration-assisted machining, the cutting motion of the tool is superimposed by a vibration with a given frequency [10]. The additional relative movement between tool and workpiece leads to changed cutting conditions and reduces process forces as well as tool wear [2]. In addition, the range of machinable materials can be expanded by using vibration-assisted machining [16], which enables applications requesting materials that could not be machined without vibration-assistance. Moreover, vibration-assisted machining is used to produce special surfaces [15], e.g. to improve wettability chracteristics [17]. With regard to micro milling processes with tool diameters of 100 µm and smaller, the use of vibration-assisted machining has not yet been investigated. However, the advantages of the reduced process forces during vibration-assisted machining and the resulting reduced deformation of the machine are promising to further increase the accuracy of the machining result. In order to give an insight into the effects of vibration-assisted machining on the production of structure sizes smaller than 1 mm, a selection of research on vibration-assisted machining with tool diameters of 400 µm and 500 µm is presented below.
In the investigations of Lian et al. [11] the effects of the vibrational amplitude during vibration-assisted micro milling of Al6061 were investigated. A change in the resulting surface roughness in dependence of the vibration's amplitude was observed. The surface roughness reached an optimum at 11 µm vibrational amplitude, which corresponds to a reduction in surface roughness by approx. 52 %. In the investigations, a double edged milling tool with d = 500 µm was used.
In the work of Noma et al. [13] the influence of vibration-assisted machining on the helical milling of glass was investigated. A diamond tool with d = 400 µm, vibrating in axial direction with a frequency of 70 kHz and an amplitude of 4 µm, was used. The investigations showed a significant decrease in process forces by 84 - 86 %. In addition, considerably less tool wear and thus increased tool life as well as a reduced chip size was observed when using vibration-assisted machining.
Supplementing these findings, in this paper the effects of vibration-assistance on micro milling using significantly smaller (d = 100 µm) and single-edged tools is investigated. The design is supported by simulations. The simulative characterization is validated and the final system is applied for the machining of brass (CuZn39Pb2). Different orientations of the feed direction and the direction of the vibration are investigated for frequencies up to 15 kHz. The influence of vibration-assistance is evaluated on the basis of process forces, surface roughness, burr formation and the slot bottom.

2 Design

In this section the requirements and specifications of the system are explained. In addition, the performance characteristics of the system are discussed.

2.1 System Requirements

The system should allow vibration in at least one coordinate direction perpendicular to the tool's axis of rotation (z-axis, see Figure 1). Excitation perpendicular to the z-axis has the advantage that it is not necessary to overcome the weight of the sample for excitation. Even with the small sample sizes in micro machining, large piezo-electric actuators are required when working against the sample's weight. Therefore, in this investigation an excitation perpendicular to the z-axis was used. By adjusting the feed direction during milling, thus the influence of the direction of the vibration on the process result can be examined. Further, the frequency of the vibration needs to be freely adjustable in order to investigate the influence of varying frequencies during vibration-assisted machining on the process results. As the system to enable vibration-assisted machining will be integrated into an already existing ultra-precision machine, the compatibility of the interfaces of both systems is of special importance. As the ultra precision machine contains a dynamometer for the recording of process forces occurring during machining, the dynamometer is defined as the interface between the machine tool and the vibration-assisting system. The interface and a summary of the system requirements are shown in Figure 1.

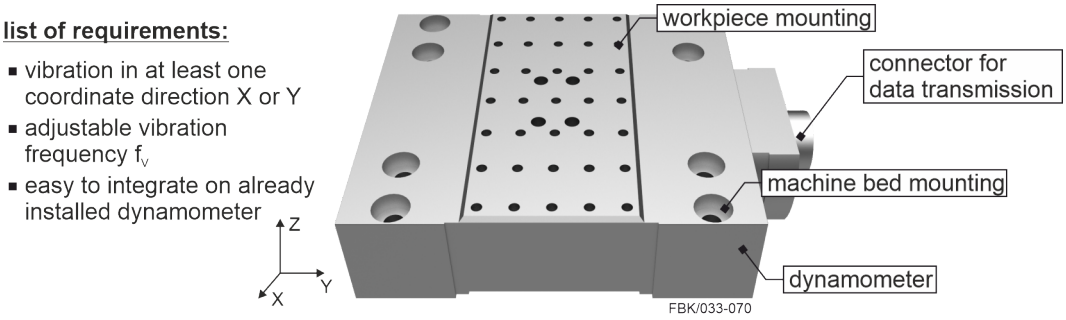

Figure 1 List of requirements and interface for which compatibility must be ensured.

2.2 System Specification

In Figure 2 the designed system to enable vibration-assisted micro milling is shown. The design is similar to the vibration systems used in [17, 9, 3].

Basis of the designed system is a frame, which is mounted directly on the dynamometer and allows an easy integration into already existing systems. On this frame the workpiece holder and the piezo-electric actuator, which generates the vibration, are attached. For the preload of the piezo and the system in general, it has been considered to use as many standard parts as possible. Therefore, the actuator is mechanically preloaded between the frame and the workpiece holder by a standard thread. The actuator's vibration frequency can be controlled via its electric connection. When the piezo-electric actuator changes its length due to an applied voltage, it deflects the workpiece holder. The stiffness of the workpiece holder was reduced in the vibration's direction (x-direction) by using solid-state joints. The modular design of the system enables a quick exchange of the workpiece holder and is not

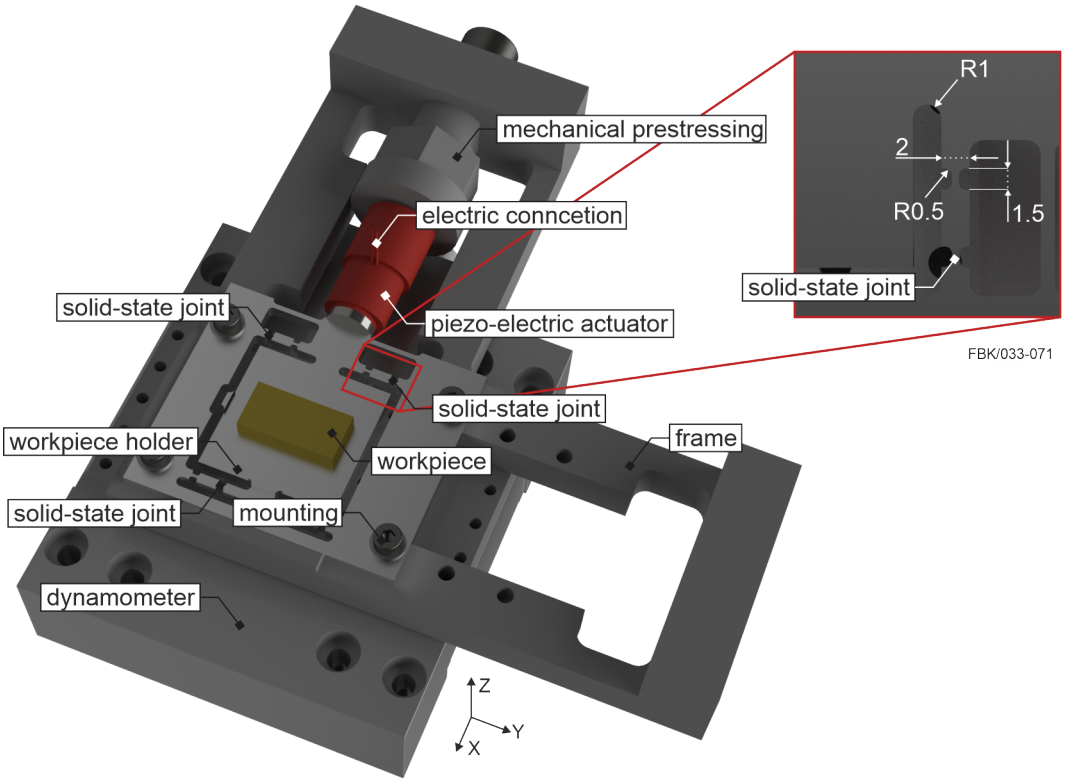

Figure 2 CAD rendered image of piezo-driven system.

bound to a specific geometry of workpiece holders. Furthermore, the system's frame is prepared for the use of a second actuator. The workpiece is attached to the workpiece holder by means of an adhesive joint.

The system is equipped with a piezo-electric ring actuator (Physik Instrumente (PI), P 010.20H PICA1[1]). The actuator is not preloaded at delivery but was mechanically preloaded in the system with 1 MPa due to the increased compressive strength of piezo-electric actuators compared to their tensile strength. The maximum travel Δl_0 of the actuator is 30 µm at an operating voltage of 1000 V. The sinusoidal electric signal to control the actuator is generated by a frequency generator (Hameg, HM 8030 31[1]) and is amplified by a controller (Physik Instrumente (PI), E 618.10G1[1], max. frequency: 15 kHz). With the system's stiffness in x-direction of 2.23 N/µm (calculated in section 3.1), this setup allows a theoretical vibrational amplitude of 1.8 µm at frequencies up to 15 kHz. Due to the low feed per tooth in micro milling of $f_z = 1$ µm and the spindle's speed of n = 24,420 min^{-1} (see section 4), the system ensures that the tool exits the material during machining and is therefore suitable for the application in vibration-assisted micro machining.

3 Finite Element Analysis

In the following the simulative characterization of the system is described by means of a convergence study for the stiffness analysis and a modal analysis. The software ANSYS Workbench 19.211 was used to run the simulations.

3.1 Stiffness Analysis

In order to calculate the maximum displacement of the piezo-electric actuator, the system's stiffness has to be known. In general, simulation results become more accurate as the mesh becomes finer. However, due to the increasing complexity of the mesh, the fineness of the mesh is directly linked to the calculation time required for the simulation. In order to determine the element size at which the simulation result is no longer subject to major changes, several simulations with varying mesh sizes need to be compared. Therefore, a study to determine the mesh's convergence was carried out. For this purpose, the stiffness of the designed system in the vibration's direction (x-direction) was calculated using Finite Element Analysis at different mesh sizes (0.4 - 4 mm). The convergence criterion was defined as a change in the simulation result of less than 3 % within three successive mesh refinements. The boundary conditions for the calculation of the static stiffness and an exemplary meshing of the workpiece holder and the workpiece with an element size of 4 mm are shown in Figure 3.

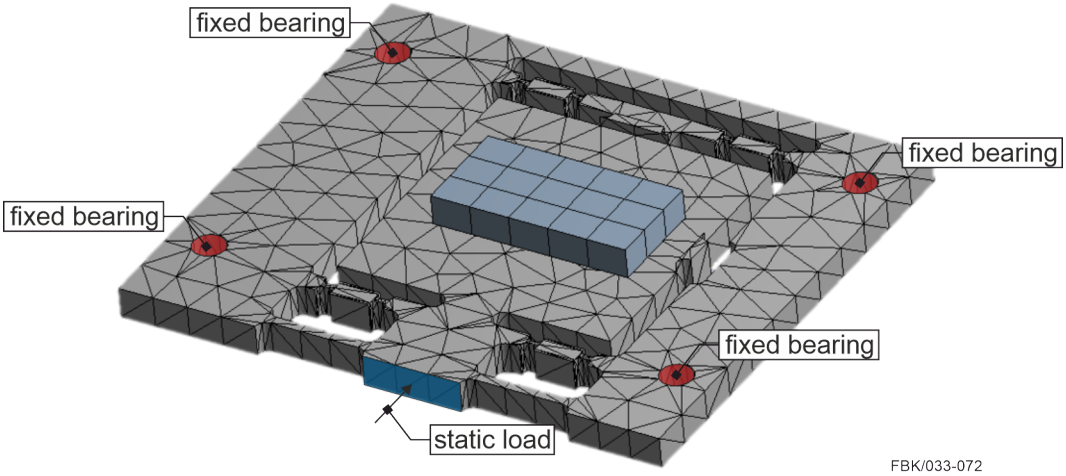

Figure 3 Boundary conditions for Finite Element Analysis and exemplary representation of the mesh with an element size of 4 mm.

The mounting holes for fixing the workpiece holder onto the frame have been defined as fixed bearings, which suppresses their movement for all degrees of freedom. As the correlation between force and deflection is linear, a static load of 10 N has been chosen as force acting on the contact surface between the piezo-electric actuator and the workpiece holder. This force leads to small deflections of the system in the single-digit micrometer range, which is similar to the system's application and thus leads to comparable conditions between simulation and reality. The stiffness of the workpiece holder was calculated by the ratio of the given force and the simulated displacement in direction of the applied force. In Figure 4 the results of the Finite Element Analsysis are given, showing the deflected workpiece holder for an element size of 4 mm. The color scale indicates the deflection in x-direction, that is, in the direction of the vibration generated by the piezo-electric actuator. The uniform coloring of the inner part of the workpiece holder shows that the kinematics of the workpiece holder allows an equal movement of the workpiece in x-direction.

In Table 1 the results of the convergence study are shown. For each simulation the element size, the number of nodes and elements of the mesh, as well as the deflection and stiffnes are shown. In addition, the percentage change in stiffness to the next larger mesh is given.

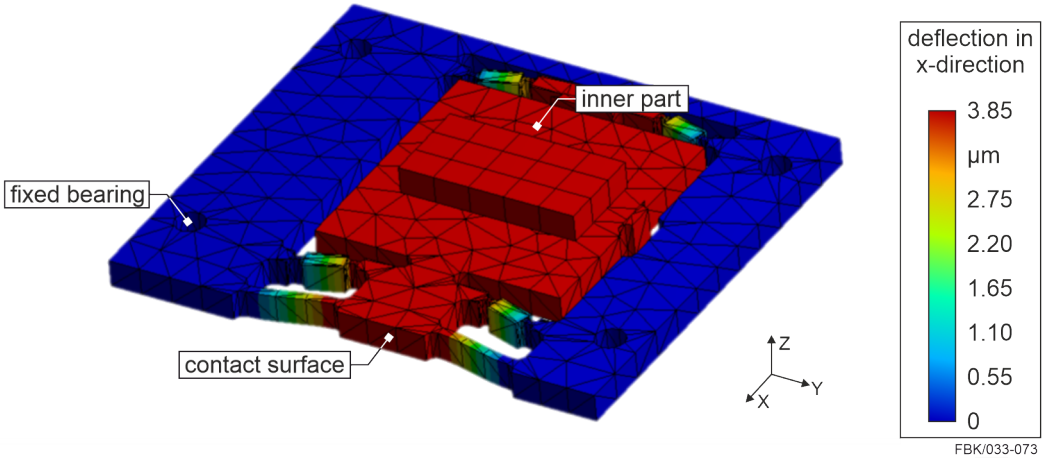

Figure 4 Deflected system shown for an element size of 4 mm.

Table 1 Simulation results of the convergence study calculating the workpiece holder's stiffness.

element size in mm	number of nodes	number of elements	deflection in µm	stiffness in N/µm	percentage change
4.0	5,800	2,630	3.83	2.61	-
3.0	8,290	3,969	3.85	2.60	-0.46 %
2.0	18,123	9,523	3.87	2.58	-0.68 %
1.0	99,538	61,806	4.18	2.39	-7.30 %
0.8	185,298	118,150	4.28	2.34	-2.36 %
0.6	411,591	271,224	4.38	2.28	-2.28 %
0.4	1,325,754	903,466	4.49	2.23	-2.45 %

The results of the mesh study show stiffness values from 2.61 - 2.23 N/µm with varying element sizes from 4 - 0.4 mm. Considering the percentage change of the stiffness, the biggest change (-7.30 %) is observed when refining the mesh's element size from 2 to 1 mm. Starting at an element size of 0.8 mm and below, however, only slight changes within the lower single digit percentage range were found in the simulation results, which complies the stop criterion and indicates that the mesh is sufficiently accurate to use the stiffness for the calculation of the actuator's displacement.

According to [12], the actuator's travel for alternating external loads Δl is given by:

$$\triangle l = \frac{\triangle l_0 \cdot c_{\mathrm{System}} - F}{c_{\mathrm{System}} + c_{\mathrm{Piezo}}} \tag{1}$$

with the actuator's maximum travel Δl_0 and the constant force of mechanical preload F. The system's stiffness c_{System} of 2.23 N/µm and the mechanical preload F are relatively low compared to the stiffness of the piezo-electric actuator (manufacturer's information: $c_{\mathrm{piezo}} = 68$ N/µm), which leads to a minor influence of the actuator's travel. Due to the controller's output voltage of 130 V and the piezo's linear operating range [8] a travel of 3.6 µm is reached, leading to a vibrational amplitude of 1.8 µm. Due to the stiffness of the solid-state joints in the direction of the vibration (x-direction), the actuator's travel and therefore the vibration's amplitude is suitable to enable vibration-assisted machining.

3.2 Modal Analysis

The travel of the piezo-electric actuator is represented by a vibration in x-direction which is transferred to the workpiece. When the actuator's vibrational frequency matches the natural frequencies, unwanted movements of the workpiece can occur. However, it is also possible to further amplify the intended movement. To anlyze this, a simulative modal analysis was carried out.

In Figure 5 the simulation results of the modal analysis are listed, which show the system's natural frequencies up to 15 kHz. Two different examples of modes that occur due to vibration in natural frequencies are illustrated. The shown deformation of the workpiece holder when vibrating in the natural frequency of 1959 Hz is identical with the movement induced by the piezo-electric actuator. Due to the positive interference between excitation vibration and natural frequency, the desired motion of the workpiece holder is enhanced which leads to an increase of the vibration's amplitude when excited with 1959 Hz and harmonics of this natural frequency. The natural frequency at 1959 Hz is the only vibration up to 15 kHz at which the modal analysis revealed an amplification of the vibration. All other natural frequencies have to be avoided.

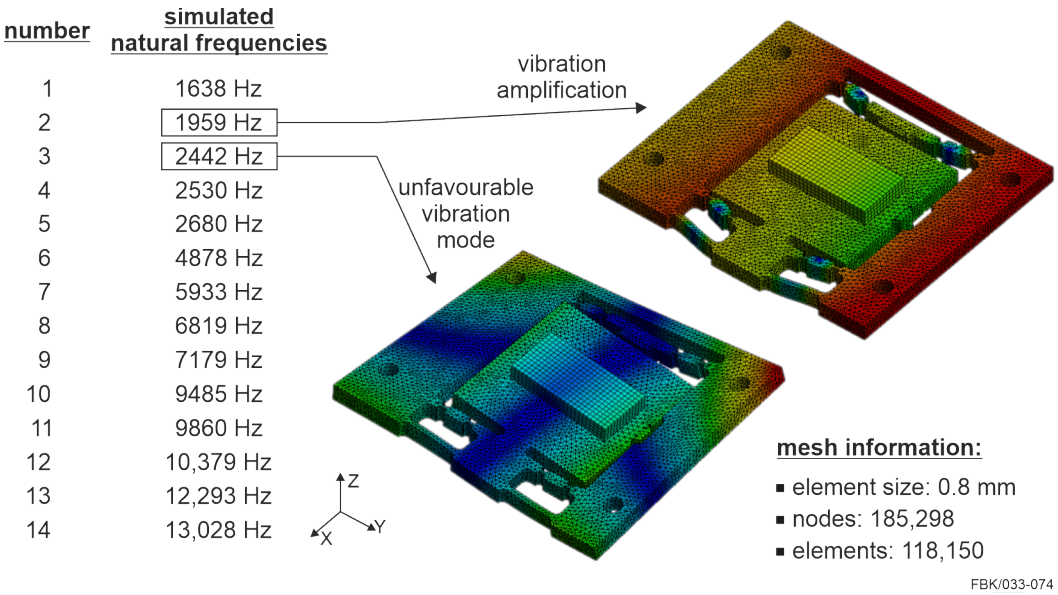

Figure 5 Simulated natural frequencies up to 15 kHz and representation of different vibration modes.

The negative influence of natural frequencies other than 1959 Hz on the system's motion is also demonstrated in Figure 5, where the mode of the natural frequency vibration at 2442 Hz is shown. It can be seen that the equal displacement in x-direction of the inner part of the workpiece holder and the workpiece itself is superimposed by numerous undesired displacements. The most significant motion in this example is a rotation around the x-axis, which causes the workpiece surface to move along the z-axis. Since the amplitudes of natural frequency vibrations are generally more intense than those of forced vibrations, it can be assumed that at this frequency only the disruptive displacement can be observed. These disruptive movements significantly disturb the accuracy of micro machining and can lead to tool breakage. The results of the modal analysis were used for the design of the experiment in order to avoid natural frequencies and to only meet the natural frequency of 1959 Hz and its harmonics at which the intended motion of the workpiece is favourably enhanced.

4 Experimental Setup

The experimental tests were performed on a LT Ultra MMC 600H[1] machine tool. This 5-axes ultra-precision milling machine features hydrostatic mounted axes. The x-, y- and z-axis are driven by linear motors, the rotary axes are driven by torque motors. The maximum rotational speed of the air bearing spindle (Levicron ASD-80-H25[1]) is 80,000 rpm. Brass CuZn39Pb3 was used as workpiece material. The workpiece (20 x 10 x 3 mm) was glued to the workpiece holder, which was mounted on the system's frame (see section 2.2). The vibration system was mounted on the Kistler 9119AA2[1] dynamometer, which was fixed to the machine tool. The workpiece was face milled in the identical clamping used for the tests prior to the vibration-assisted experiments. All experiments were carried out using one workpiece and clamping in order to avoid changes of the system's natural frequencies due to smallest variations of the piezo's mechanical preload or the workpiece's mass and position during re-clamping. The experimental setup is shown in Figure 6a.

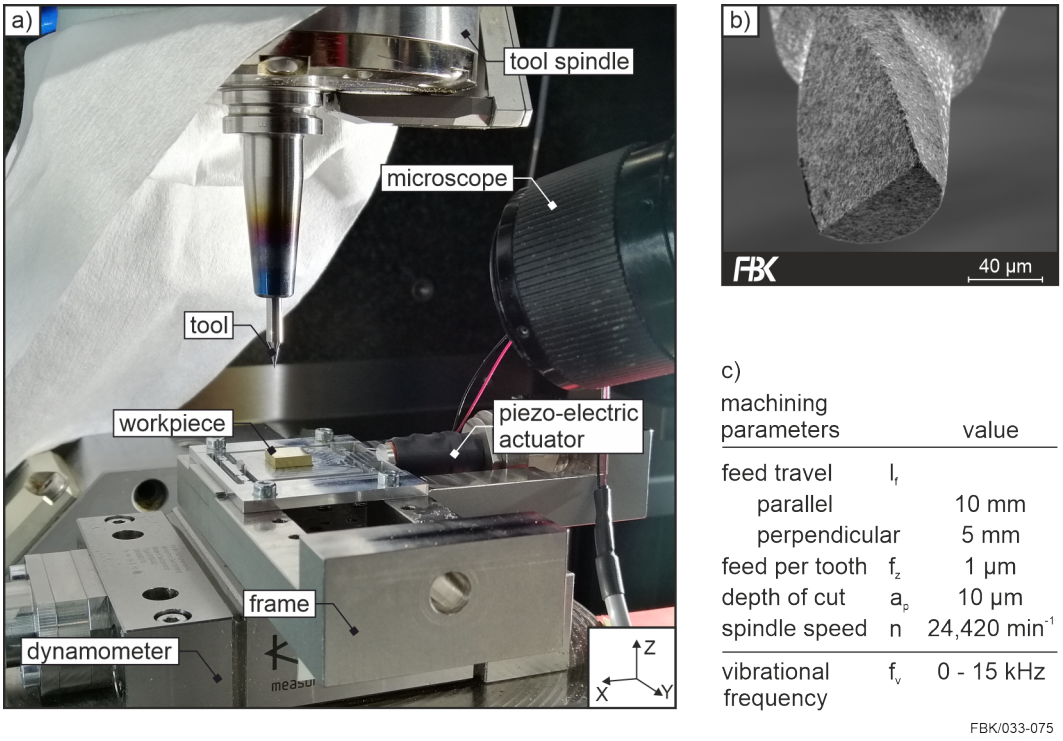

Figure 6 a) Experimental setup, b) micro milling tool, c) cutting parameters.

A single-edged cBN-tool (NS tools; SMEZ120 D0,100[1]) with an effective radius of 50 µm was used for machining (see Figure 6b). This tool was clamped in a Levicron HSW-E[1] shrink chuck: the static concentricity error is below 0.8 µm (manufacturer's specification). All experiments were carried out without metalworking fluid. The process was monitored with a microscope camera. When choosing the spindle speed, it must be ensured that it does not coincide with the frequencies to be tested. If the two frequencies were equal, they could not be distinguished from each other in the force signal within the frequency analysis (Fourier transformation of the force signal, see section 5.1). Thefore, the spindle speed was set to 24,420 rpm, which corresponds to 407 Hz and does not coincide with any of the excitation frequencies (see Table 2). Due to the superposition of the tool's cutting movement and the

workpiece's vibration, the number of oscillations between tool and workpiece per rotation m is given by the ratio of the vibration's frequency to the spindle's rotational frequency:

$$m = \frac{f_{\mathrm{v}} \cdot 60}{n} \tag{2}$$

The frequencies of the vibrations examined were defined as follows: The process forces were monitored in real time. Only the offset (tool not engaged) of the force was recorded. The sample was vibrated with the described setup and operated at frequencies of 0 - 15 kHz. The frequency at which the force offset became maximum was detected. At this frequency, a natural frequency or a harmonic of a natural frequency is to be assumed, which causes the workpiece holder to vibrate. The frequency detected with this method, generating the largest vibration, was about 3.8 - 3.9 kHz. This experimentally determined frequency corresponds to twice the natural frequency (1st harmonic) at which the simulation showed an amplification of the desired motion by the vibration. At the natural frequency an amplification of the oscillation was also noticed, but the intensity was lower than at the first harmonic. The frequency area around the resonance frequency (3.8 - 3.9 kHz) was investigated more closely in the subsequent test, the tests without excitation and with excitation at the resonance frequency were repeated three times for statistical verification (see Table 2).

Table 2 Tested frequencies of vibration-assisted micro milling.

Tested frequency of vibration in kHz	Number of oscillations per spindle rotation m	Repetitions for statistical verification
0	0	3
1	2.5	1
2	4.9	1
3	7.4	1
3.6	8.8	1
3.7	9.1	1
3.8	9.3	3
3.9	9.6	3
4.0	9.8	1
5.0	12.3	1
6.0	14.7	1
10.0	24.6	1
15.0	36.9	1

The maximum sampling rate of the force measurement using the dynamometer was 12 kHz. Due to the fact that the sampling rate according to the Nyquist theorem must be more than twice the vibration's frequency, a frequency analysis of the measured process forces is only possible up to 6 kHz. Accordingly, only two frequencies above 6 kHz were tested.

During the test, slots were milled either parallel or perpendicular to the direction of vibration (see Figure 7). The vibration was carried out in the same direction in all experiments, according to the design of the workpiece holder described in section 2.2. Therefore, the feed direction was adjusted accordingly to realize both cases (parallel and perpendicular to the vibration's direction). The feed travels for the slots are listed in Figure 6c. The different lengths of feed travels were chosen to avoid the crossing of slots milled with different feed direction.

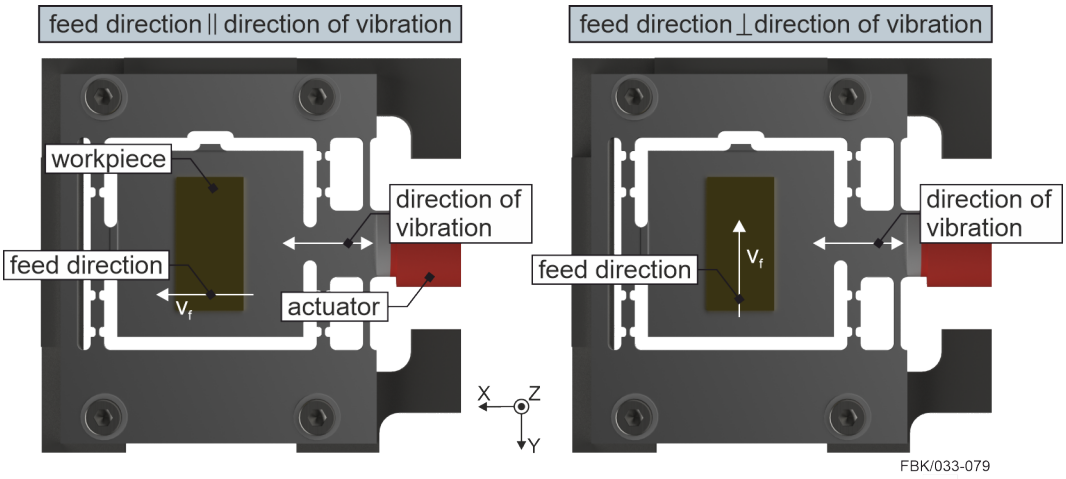

Figure 7 Variation of the feed direction in relation to the direction of vibration.

After machining, all slots were characterized with a confocal microscope (Nanofocus µSurf explorer[1]). The objective used features a 50x magnification and a numerical aperture of 0.5. In order to determine the areal surface texture parameters, three images were taken per slot: one image at the beginning of the slot, one in the middle of the slot and one image at the end of the slot. The measuring field of the three images corresponded to a single field size of the objective used (320 µm x 320 µm). In addition to the areal analysis, a profile analysis was also carried out. For this purpose, a larger measuring field, which was stitched from two single fields, was measured in the middle of each slot. One profile section in the middle of the slots was taken from this larger measuring field for the profile evaluation. The processing of the data was carried out in MountainsMap[1] as follows for the areal and profile evaluation:

Areal surface texture parameters

- Untilting of the measured data (fitting of a plane)
- Extraction of the evaluation area: size: 75 µm (width) x 100 µm (length). Not the entire width of the slot was extracted since burr partially protruded into the slot. In order to eliminate this area for evaluation, only a width of 75 µm was used. This central area was extracted in the same way for all slots.
- Filtering: ls = 0.25 µm
- Calculation of the surface texture parameter Sa according to ISO 25178-2 [6]

Profile roughness parameters

- 480 µm long profile is extracted in the middle of the slot
- Filtering: ls = 0.25 µm and lc = 8 µm
- Calculation of the roughness parameter Ra according to ISO 4287 [5]

In order to qualitatively examine the resulting topographies at the slot bottoms and the burr formation, scanning electron microscope (SEM) images were taken in addition to the described measurements with the confocal microscope.

During machining, the process forces were detected with a dynamometer (Kistler 9119AA2[1]). The recorded process forces were then evaluated in Matlab[1]. First, long-wavelength components, which can be caused by drifts, were filtered out. A high-pass

filter with a cut-off frequency of 1 Hz was used. Then the offset of the recorded forces was determined. This offset contained the inertial forces resulting from the vibration of the inner part of the workpiece holder and the workpiece itself when the tool is not in engagement. The offset was subtracted from the total force to determine the force acting on the tool. The evaluated resultant force value is derived from the mean length value of the vector addition of the measured forces in x-, y- and z-direction. The specific resultant forces were calculated by determining the individual slot depths and the ratio between force to individual slot depth.

5 Experimental Results

The simulative characterization of the system via the modal analysis (section 3.2) was validated experimentally. Subsequently, vibration-assisted micro milling was done for several vibrational frequencies with feed direction parallel and perpendicular to the direction of vibration. The experimental results were evaluated on basis of the process forces, the surface roughness, the burr formation and the slot bottom quality.

5.1 Vibration Analysis

In Figure 8 a linear interpolation of the results of the Fourier transformation (FFT) of the force signal in the direction of the vibration (x-direction) is shown for vibration frequencies between 0 - 6 kHz.

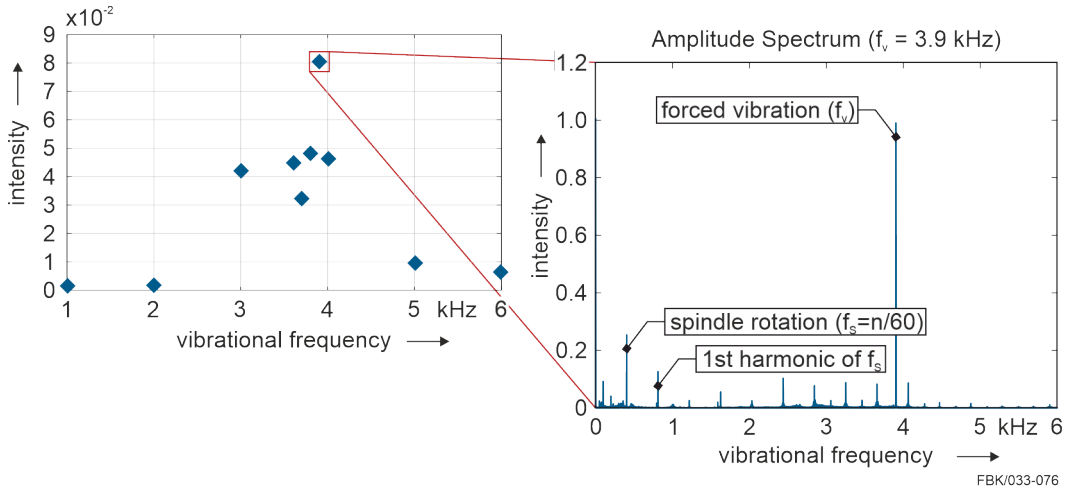

Figure 8 Measured system response to forced vibration and amplitude spectrum for $f_v = 3.9$ kHz.

The average deviation between the frequency set at the frequency generator and the measured frequency (x-coordinate of the forced vibration in the FFT, see Figure 8) was 0.2 %. The intensity of the vibrations determined during tool engagement show a clear peak at $f_v = 3.9$ kHz. As described in section 4, a significant increase of the inertial forces in the direction of the vibration was observed at this frequency. This resonant frequency can be assumed to be the 1st harmonic of the systems natural frequency at 1959 Hz (see section 3.2). Since the real time monitoring of forces showed that the resonance at $f_v = 3.9$ kHz was more intense than the resonance at the natural frequency, vibration-assistance at this resonance frequency causes the strongest amplification of the system's vibrational amplitude. In addition to the intensities of the vibrations generated by the piezo-electric actuator, the detailled

amplitude spectrum at the vibrational frequency of $f_v = 3.9$ kHz is also given in Figure 8. The analysis of the spectrum shows two vibrations that are particularly distinctive. One of these two vibrations is due to the spindle's rotation at $f_S = n/60 = 407$ Hz. The peaks that repeat at regular intervals are harmonics of f_S and can also be attributed to the vibration caused by the spindle's rotation. The most distinctive vibration in the shown amplitude spectrum is the vibration at f_v which is generated by the piezo-electric actuator. The comparison of the intensities shows that the vibration at f_v clearly exceeds that of the spindle's vibration. The high intensity is due to f_v meeting the 1st harmonic of the workpiece holder's natural frequency at 1959 Hz, which leads to a resonance of the system and an amplification of the mode of motion of this natural frequency. The actual resonance frequency deviates by less than 1 % from results of the modal analysis. The results of the modal analysis are therefore considered validated. As this mode of motion equals the workpiece holder's motion generated by the piezo-electric actuator, it can be assumed that the amplitude during vibration-assisted micro milling is significantly increased at $f_v = 3.9$ kHz.

5.2 Process Forces

In Figure 9a the specific resultant forces are shown for the feed direction parallel and perpendicular to the direction of vibration and for varying vibrational frequencies f_v. In general, the profiles of the forces are very similar. However, slightly increased forces are observed when the feed direction is perpendicular to the direction of vibration. During micro milling specific resultant forces between 0.0016 - 0.0044 N/µm for feed direction parallel to the direction of vibration and 0.0026 - 0.0056 N/µm for feed direction perpendicular to the direction of vibration were detected.

During micro milling without vibration ($f_v = 0$ Hz) no dependence of the specific resultant forces on the feed direction was observed which is due to the non-existent vibration and the therefore identical process independent from the feed direction. The slightly increased forces when micro milling with $f_v > 0$ Hz and feed direction perpendicular to the vibration's direction is due to the orientation of these directions. When micro milling with feed direction

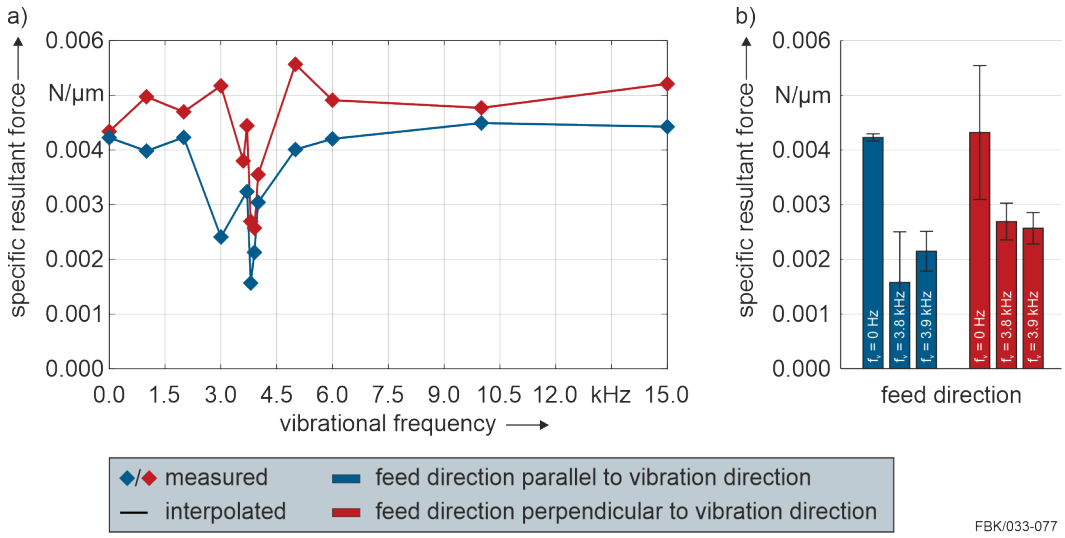

Figure 9 a) Specific resultant forces as function of vibrational frequency, b) comparison resultant force without vibration-assistance and at natural frequency for both feed directions.

perpendicular to the direction of vibration, the vibration leads to an increase of the micro milled slot's width, which results in an increased material removal and therefore increased forces. During micro milling with feed direction perpendicular to the direction of vibration and $f_v = 3.9$ kHz, an increase of the slot's width by approx. 2 µm compared to $f_v = 0$ Hz was observed. However, the measurement is interfered by burrs protruding into the slot, which can lead to deviations of the determined absolute value and the calculated amplitude of the vibration (see section 3.1). In Figure 9b the specific resultant forces and standard deviations for micro milling without vibration-assistance and with vibration in the range of the 1st harmonic of the workpiece holder's natural frequency are shown for both feed directions.

A reduction of the resultant forces during vibration-assisted micro milling is confirmed for both feed directions. Micro milling with $f_v = 0$ Hz and feed direction perpendicular to the direction of vibration shows large variations of the forces compared to the identical process with feed direction parallel to the direction intended for vibration-assistance. These differences in resultant forces are attributed to the workpiece holder's comparatively low stiffness in x-direction due to the solid-state joints. This reduced stiffness causes that the solid-state joints of the workpiece holder allow minimal movements of the workpiece perpendicular to the feed direction due to the process forces during micro milling without vibration. During vibration-assisted micro milling with vibrational frequencies $f_v > 0$ Hz the solid-state joint's displacement is defined by the vibration which avoids such undesired movements. As the feed of the tool preloads the solid-state joints of the workpiece holder when micro milling with $f_v = 0$ Hz and feed direction parallel to the intended direction of vibration, the effect of reduced stiffness during micro milling without vibration cannot be observed, which is also expressed in the significantly lower standard deviations.
Both feed directions show a strong decrease in resultant forces in the range of 3.8 - 3.9 kHz, in which the 1st harmonic of the workpiece holder's natural frequency of 1959 Hz is located. Comparing vibration-assisted micro milling at this resonant frequency to micro milling without vibration ($f_v = 0$ Hz), resultant forces were reduced by 63 % for the feed direction parallel to the direction of vibration and 41 % for the feed direction perpendicular to the direction of vibration. The lower level of resultant forces during micro milling with vibration-assistance is also given in Figure 10, showing the moving average of 1200 values of the resultant force over the corresponding process time. The maximum resultant forces for micro milling with vibration-assistance are significantly lower (0.046 N) compared to micro milling without vibration-assistance (0.070 N), which reduces the risk of tool breakage due to short-term high loads during machining.

This reduction of the forces is assumed to be due to the resonance of the workpiece holder in this frequency range, which leads to a significantly increased vibrational amplitude and thus higher velocity of the workpiece during vibration. If the speed due to the vibration exceeds the feed speed, the machining is governed by an interrupted cut [2]. We believe that this strong increase in vibrational amplitude leads to a reduced time of tool engagement which reduces the process forces. The relatively lower decrease in process force during micro milling with feed direction perpendicular to the direction of vibration compared to micro milling with feed direction parallel to the direction of vibration is due to the superposition of the increased slot width at $f_v = 3.9$ kHz compared to $f_v = 0$ Hz. As the resonant frequency of the system is no longer excited with increasing vibrational frequency and hence the amplitude of the workpiece's vibration decreases again, the cutting forces increase for $f_v > 3.9$ kHz.

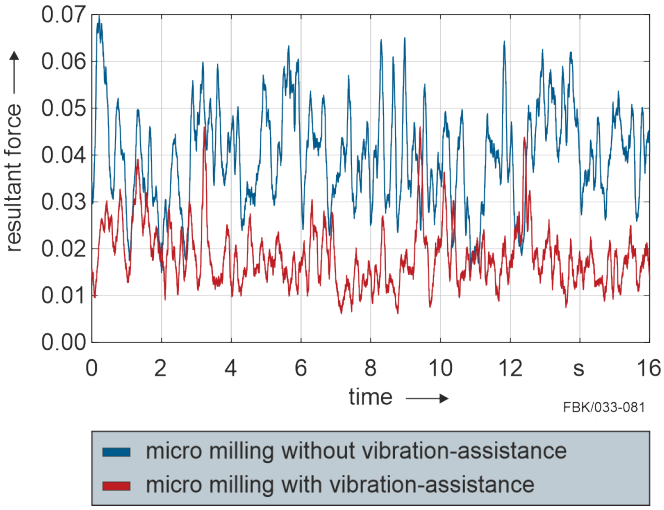

Figure 10 resultant forces with vibration-assistance (f_v = 3.9 kHz) and without vibration-assistance.

5.3 Surface Roughness

Figure 11a shows the trend of the areal surface texture parameter Sa for the different vibrational frequencies. The measured data points in the diagram represent the mean values based on the three individual measurements (beginning, middle and end of the slots). The given average standard deviation $\bar{\sigma}$ are the mean values of the standard deviation of all measurements for the respective feed direction. In Figure 11b the values of the profile roughness parameter Ra for selected vibrational frequencies are given. Here, only slots which were manufactured without vibration and slots which were manufactured with vibration at the resonance frequency are depicted. For each of these two special cases three slots were manufactured (see section 4). Each of the three slots was measured and evaluated as described, so that for each bar shown in Figure 11b nine measured values were considered (three manufactured slots, each measured at three positions). The scattering between the individual slots was displayed as error bars.

On basis of the integral parameter Sa, no trend with regard to the surface roughness as a function of the vibrational frequency can be identified when the feed direction is perpendicular to the vibration direction. The behavior is different when the feed direction is oriented parallel to the direction of the vibration. It can be figured out that the value of Sa decreases with increasing vibrational frequency and then remains at a constant level from a frequency of 6 kHz. In the range of the resonant frequency, a local maximum can be detected. However, at this point the roughness is still below the roughness for the slots that were milled without vibration-assistance. The varying roughness depending on the feed direction could be due to cutting mechanisms that occur at the slot's bottoms during machining. When the feed direction is perpendicular to the direction of vibration, the slot is wider, however, the vibration seems to have no significant influence on the kinematic roughness at the slot's bottom. Based on these observations, we believe that vibration-assisted machining with the direction of the vibration being parallel to the feed direction improves the surface quality by increasing the distance between two adjacent milling tracks and thus reducing the kinematic roughness. In addition, the feed rate is varied by the vibration which could lead to a reduction of the area at the edge of the micro milled slots where the minimum chip thickness is not reached anymore.

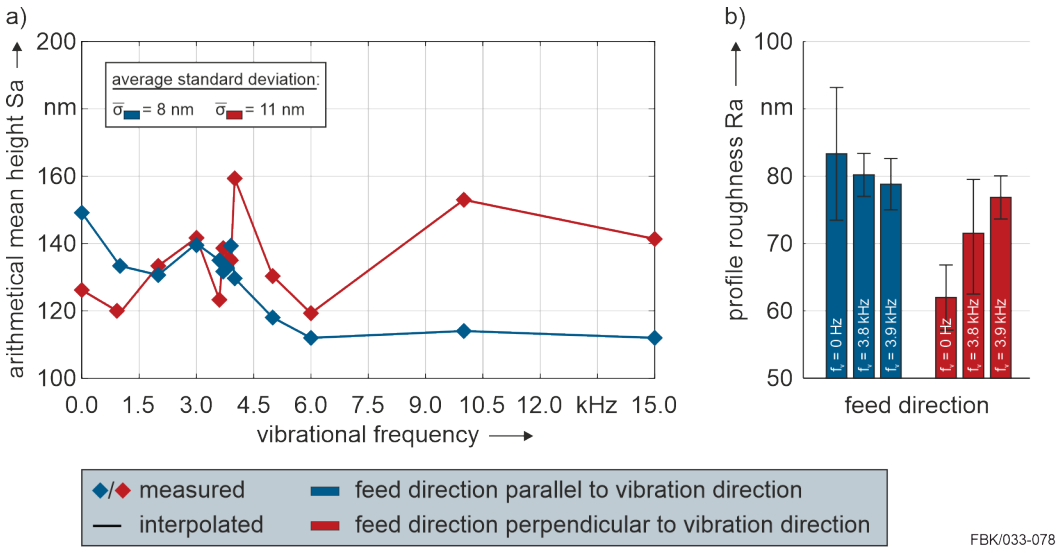

Figure 11 a) Arithmetical mean height Sa as function of vibrational frequency, b) comparison of profile roughness Ra without vibration-assistance and at resonance frequency for both feed directions.

However, the reduction of roughness does not apply to the frequency range of resonance, which is why we assume that there are overlaying effects caused by the significant increase of the vibration's amplitude. For the slots which were manufactured with feed direction parallel to the vibration's direction, a reduction of roughness when micro milling with f_v in the range of the workpiece holder's resonance can also be seen for the profile roughness parameter Ra. The values for Ra are slightly smaller in the case of vibration-assistance. The less significant reduction of Ra compared to the area based Sa may be due to the sole consideration of the profile in the middle of the slot and the neglection of areas near the slot's edge, highlighting the influence of the minimum chip thickness at the sides of the slot. It is also noticeable that most of the error bars for the slots, which were manufactured with vibration, are significantly smaller than those which were manufactuered without vibration. This means that the three successively manufactured slots exhibit only small deviations from each other in terms of their profile roughness. Vibration-assistance parallel to the feed direction thus apparently also has a positive effect on the repeatability with regard to integral roughness parameters.

5.4 Burr Formation and Slot Bottom

Figure 12 shows the burr formation and the surface of the slot bottoms for manufacturing without vibration-assistance, manufacturing with vibration at the resonant frequency and for manufacturing at the highest frequency investigated in this research. Two SEM images are shown for each slot: the image with the smaller magnification is suitable for assessing the burr formation, the image with the higher magnification shows the slot bottoms.

Solely the images in the first row (no vibration-assistance, $f_v = 0$ Hz) show slight differences in burr formation. These differences could be due to the reduced stiffness of the workpiece holder perpendicular to the feed direction (y-direction), similar to the scattering of the process forces during micro milling with feed direction perpendicular to the direction of the intended vibration. For $f_v > 0$ Hz, neither with regard to burr formation nor to the surface quality at the slot bottoms, the SEM images show any trend in dependence on the feed direction or vibrational frequency. For vibration-assisted micro milling with feed direction

parallel to the direction of vibration, no differences in burr formation and slot bottoms were found compared to $f_v = 0$ Hz. For $f_v > 0$ Hz, the workpiece holder's movement is defined by the vibration and no differences due to the feed direction could be detected. Based on these results it can be assumed that vibration-assistance has no influence on the burr formation during micro milling. Since the quantitative differences in surface roughness are in the low two-digit nanometer range (see section 5.3), there are no significant differences with regard to the surface quality in the slot bottoms when comparing the SEM images qualitatively.

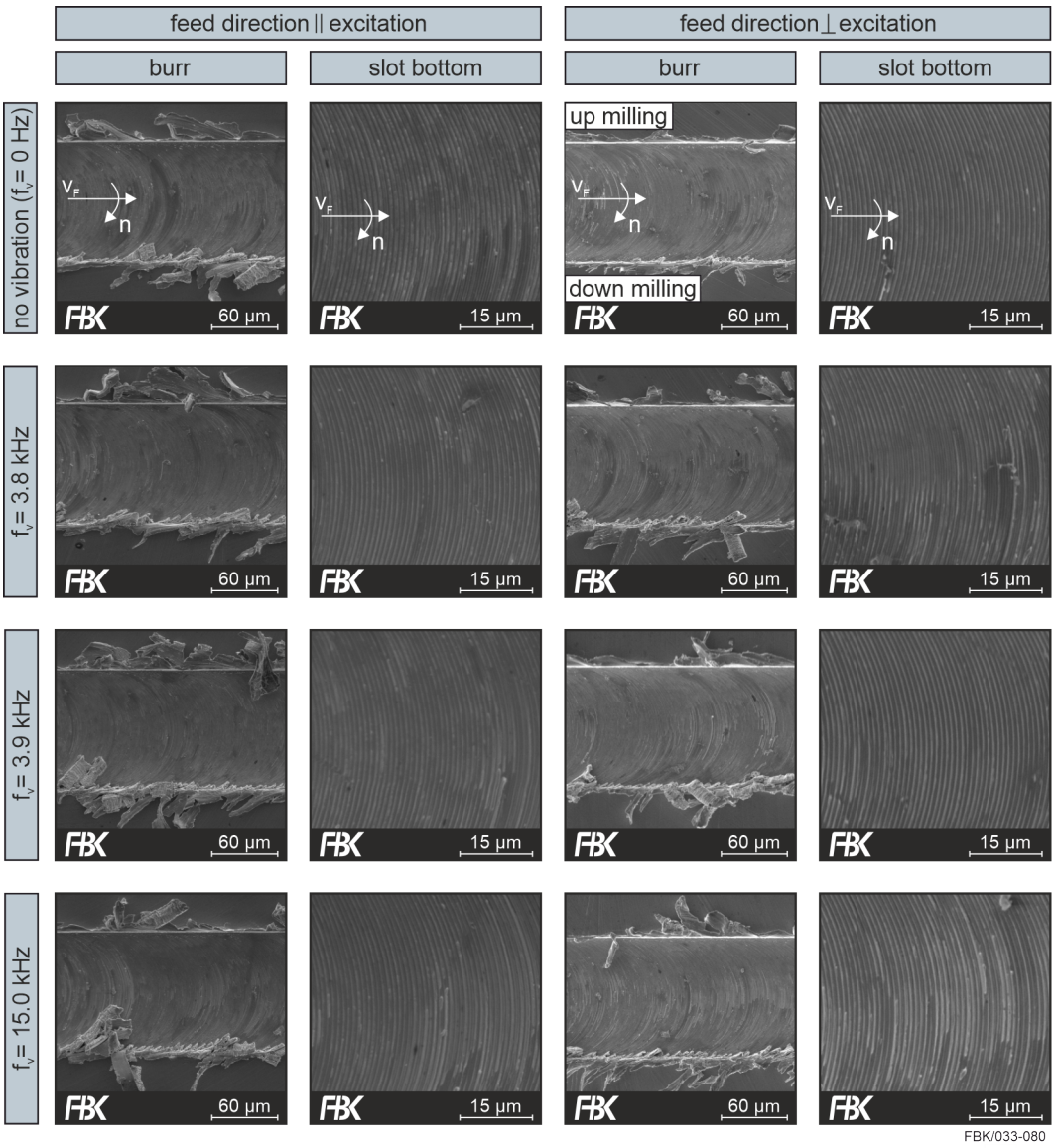

Figure 12 SEM-images of the micro milled slots showing burr and slot bottom for varying feed directions and excitation frequencies.

6 Conclusion

The research presented in this paper focused on the simulation and application of a piezo-driven system to enable vibration-assisted micro milling. In order to calculate the maximum amplitude of the vibration, the stiffness of the system in direction of the vibration was determined using Finite Element Analysis. Furthermore, the natural frequencies of the system were determined by a simulative modal analysis and vibration amplifying frequencies were identified. The system was applied for vibration-assisted machining of brass (CuZn39Pb2) with vibrational frequencies from 0 - 15 kHz. The simulative determination of the system's natural frequencies was validated by a Fourier transformation (FFT) of the force signal. The influence of vibration-assistance on micro milling was evaluated on the basis of process forces, surface roughness, burr formation and the slot bottom quality. Based on the experimental results, the following conclusions were drawn:

- Vibration in the resonant range of the system leads to a strong increase in the vibrational amplitude and a significant reduction in the process forces due to a reduced time of tool engagement.
- The orientation of the feed direction to the direction of the vibration influences the surface roughness. When these run parallel, the roughness at the slot's bottom is reduced; when these are oriented perpendicular to each other, no significant influence on the roughness was observed.
- With regard to the slot bottom appearance and burr formation evaluated via SEM-images, no difference was found between vibration-assisted micro milling and micro milling without superimposed vibration.

In future investigations the system will be extended by a second piezo-electric actuator in order to enable the superposition of two individual vibrations and to investigate the influence of bidirectional vibration-assistance on micro milling. In addition, since the reduction of process forces is the most pronounced effect of vibration-assistance observed in this investigation and leads to lower tool wear, tool wear during micro milling with increased material removal rates using vibration-assistance will be studied.

[1]Naming of specific manufacturers is done solely for the sake of completeness and does not necessarily imply an endorsement of the named companies nor that the products are necessarily the best for the purpose.

References

1 J.C. Aurich, I.G. Reichenbach, and G.M. Schüler. Manufacture and application of ultra-small micro end mills. *CIRP Annals - Manufacturing Technology*, 61(1):83–86, 2012.

2 D.E. Brehl and T.A. Dow. Review of vibration-assisted machining. *Precision Engineering*, 32:153–172, 2008.

3 W. Chen, L. Zheng, X. Wenkun, K. Yang, and D. Huo. Modelling and experimental investigation on textured surface generation in vibration-assisted micro-milling. *Journal of Materials Processing Technology*, 266:339–350, 2019.

4 D. Dornfeld, S. Mina, and Y. Takeuchi. Recent advances in mechanical micromachining. *CIRP Annals - Manufacturing Technology*, 55(2):745–768, 2006.

5 DIN e.V. *DIN EN ISO 4287:2010-07, Geometrische Produktspezifikationen (GPS) – Oberflächenbeschaffenheit: Tastschnittverfahren – Benennungen, Definitionen und Kenngrößen der Oberflächenbeschaffenheit.* Beuth Verlag, 2010.

6 DIN e.V. *DIN EN ISO 25178-2, Geometrische Produktspezifikationen (GPS) – Oberflächenbeschaffenheit: Flächenhaft – Teil 2: Begriffe und Oberflächen-Kenngrößen.* Beuth Verlag, 2012.

7 X. Gao, B. Li, J. Hong, and J. Guo. Stiffness modeling of machine tools based on machining space analysis. *International Journal of Advanced Manufacturing Technology*, 86(5-8):2093–2106, 2016.

8 K. Janschek. *Systementwurf mechatronischer Systeme.* Springer-Verlag, 2010.

9 X. Jin and B. Xie. Experimental study on surface generation in vibration-assisted micro-milling of glass. *International Journal of Advanced Manufacturing Technology*, 81:507–512, 2015.

10 M.N. Kuma, S.K. Subbu, P.V. Krishna, and A. Venugopal. Vibration assisted conventional and advanced machining: A review. *Procedia Engineering*, 97:1577–1586, 2014.

11 H. Lian, Z. Guo, Z. Huang, Y. Tang, and J. Song. Experimental research of al6061 on ultrasonic vibration assisted micro-milling. *Procedia CIRP*, 6:561–564, 2013.

12 T. Melz. *Entwicklung und Qualifikation modularer Satelitten-Systeme zur adaptiven Vibrationskompensation an mechanischen Kryokühlern.* Technische Universität Darmstadt, 2001.

13 K. Noma, Y. Takeda, T. Aoyama, Y. Kakinuma, and S. Hamada. High-precision and high-efficiency micromachining of chemically strengthened glass using ultrasonic vibration. *Procedia CIRP*, 14:389–394, 2014.

14 I. G. Reichenbach, M. Bohley, F. J. Sousa, and J. C. Aurich. Tool-life criteria and wear behavior of single-edge ultra-small micro end mills. *Precision Engineering*, 55:48–58, 2019.

15 D. Xing, J. Zhang, X. Shen, Y. Zhao, and T. Wang. Tribological properties of ultrasonic vibration assisted milling aluminium alloy surfaces. *Procedia CIRP*, 6:539–544, 2013.

16 L. Zheng, W. Chen, and D. Huo. Review of vibration devices for vibration-assisted machining. *International Journal of Advanced Manufacturing Technology*, 108(5-6):1631–1651, 2020.

17 L. Zheng, W. Chen, M. Pozzi, X. Teng, and D. Huo. Modulation of surface wettability by vibration assisted milling. *Precision Engineering*, 55:179–188, 2019.